



## In situ FT-infrared investigation of CO or/and NO interaction with CuO/Ce<sub>0.67</sub>Zr<sub>0.33</sub>O<sub>2</sub> catalysts

Lianjun Liu<sup>a</sup>, Bin Liu<sup>a</sup>, Lihui Dong<sup>a</sup>, Jie Zhu<sup>a</sup>, Haiqin Wan<sup>a</sup>, Keqin Sun<sup>b</sup>, Bin Zhao<sup>a</sup>, Haiyang Zhu<sup>a,\*</sup>, Lin Dong<sup>a,\*</sup>, Yi Chen<sup>a</sup>

<sup>a</sup>Key Laboratory of Mesoscopic Chemistry of MOE, School of Chemistry and Chemical Engineering, Nanjing University, Hankou Road 22#, Nanjing 210093, Jiangsu, PR China

<sup>b</sup>Jiangsu Suyuan Environmental Protection Engineering Co. Ltd, No. 58 Su Yuan Rd, Jiangning District, Nanjing 211102, PR China

### ARTICLE INFO

#### Article history:

Received 26 September 2008

Received in revised form 13 April 2009

Accepted 16 April 2009

Available online 23 April 2009

#### Keywords:

CuO–CZ catalysts

In situ FT-IR

CO or/and NO interaction

Nitrites/nitrates

### ABSTRACT

In situ FT-IR was employed to investigate CO or/and NO interaction with CuO supported on Ce<sub>0.67</sub>Zr<sub>0.33</sub>O<sub>2</sub> (hereafter denoted as CZ) catalysts. The physicochemical properties of CuO–CZ were also studied by combination of XRD, TPR and NO + CO activity tests. The results indicated that the dispersed CuO species were the main active components for this reaction. The catalysts showed different activities and selectivities at low and high temperatures, which should be resulted from the reduction of dispersed copper oxide species. This reaction went through different mechanisms at low and high temperatures due to the change of active species. FT-IR results suggested: (1) CO was activated by oxygen originating from CZ support, which led to surface carbonates formation, and partial dispersed CuO was reduced to Cu<sup>+</sup> species above 150 °C; (2) NO interacted with the dispersed CuO and formed several types of nitrite/nitrate species, whereas crystalline CuO made little contribution to the formation of new NO adsorbates; (3) NO was preferentially adsorbed on CuO–CZ catalysts compared with CO in the reactants mixture. These adsorbed nitrite/nitrate species exhibited different thermal stability and reacted with CO at 250 °C. As a result, a possible mechanism was tentatively proposed to approach NO reduction by CO over CuO–CZ catalyst.

© 2009 Elsevier B.V. All rights reserved.

## 1. Introduction

The reduction of NO by CO is one of the important reactions for exhaust gas depollution and numerous catalysts have been attempted to approach this reaction process. Noble metal catalysts containing Pt, Pd and Rh have attracted much attention due to their high activity and selectivity. Several IR studies were also carried out to investigate the NO reduction by CO over these supported noble metal catalysts [1–8].

Recently, transition metal oxides contained catalysts, particularly copper oxide supported on Al<sub>2</sub>O<sub>3</sub> and CeO<sub>2</sub>, have also been investigated for NO reduction to replace the noble metal catalysts due to their high costs, limited thermal stability and poor resistance to sulfur [9–19]. It was well documented that the performance of these copper-based catalysts was influenced by the support due to the strong interaction between active copper species and support. Ceria–zirconia solid solution, as the

support, combined the advantages of ceria and zirconia, i.e., strong oxygen storage and release capacity and high thermal stability [20–23]. Ceria–zirconia solid solution with the Ce/Zr molar ratio of 2:1 exhibited favorable redox properties and excellent thermal stable structure [24–26]. Hence, ceria–zirconia solid solution was considered as a potential support for the catalysts in the NO removal reaction. However, the researches about copper oxide supported on ceria–zirconia solid solution and its application in the NO reduction by CO were very limited, and the interaction between dispersed copper oxide species and ceria–zirconia solid solution as well as the reactants (CO and NO) with CuO–CZ was not clear yet, which was the focus of this work.

In the present study, CuO–CZ catalysts were characterized by XRD, TPR, in situ FT-IR, and the activity for NO reduction by CO was also tested to (1) explore the interaction between copper oxide and ceria–zirconia solid solution, (2) investigate the interaction of CO or/and NO with these catalysts. The correlation between the reducibility of highly dispersed copper oxides and their catalytic activities also appeared to be discussed. These results would be helpful for understanding the NO reduction by CO over copper oxide supported on CZ catalyst.

\* Corresponding author. Tel.: +86 25 83594945; fax: +86 25 83317761.

E-mail addresses: [haiyangz79@gmail.com](mailto:haiyangz79@gmail.com) (H. Zhu), [donglin@nju.edu.cn](mailto:donglin@nju.edu.cn) (L. Dong).

## 2. Experimental

### 2.1. Catalysts preparation

In this work, CZ solid solution was synthesized following the procedure of Li et al. [27]. A requisite amount of  $(\text{NH}_4)_2\text{Ce}(\text{NO}_3)_6 \cdot 6\text{H}_2\text{O}$  and  $\text{Zr}(\text{NO}_3)_4 \cdot 5\text{H}_2\text{O}$  were dissolved in distilled water, and the excess ammonia was slowly dropped to the mixture solution with vigorously stirring until  $\text{pH} = 10$ . The resulting solution was kept in stirring for another 3 h, aged overnight and then filtered, washed with distilled water until no pH change. The obtained solid sample was first dried at  $110^\circ\text{C}$  overnight and then calcined in a muffle stove at  $500^\circ\text{C}$  in flowing air for 4 h.  $\text{CeO}_2$  and  $\text{ZrO}_2$  were prepared via the same method. The surface area of CZ support was  $121.78 \text{ m}^2/\text{g}$ , which was determined via nitrogen adsorption at  $77 \text{ K}$  with the Brunauer–Emmet–Teller (BET) method using a Micrometrics ASAP-2000 adsorption apparatus.

The CuO–CZ catalysts were prepared by incipient-wetness impregnating the support with the solution containing  $\text{Cu}(\text{NO}_3)_2$ . The mixture was kept vigorously stirring for 3 h, and then evaporated at  $100^\circ\text{C}$ . The resulting materials were dried at  $110^\circ\text{C}$  overnight and then calcined in a muffle stove at  $500^\circ\text{C}$  in flowing air for 4 h. The CuO loadings were 0.33, 0.66, 1.23, 1.65 mmol/100  $\text{m}^2$  CZ. The catalyst was denoted as  $x\text{Cu-CZ}$ , where the “ $x$ ” indicated the loading of copper oxide.

### 2.2. Catalysts characterization

#### 2.2.1. In situ FT-IR adsorption measurement (FT-IR)

FT-IR spectra were operated at room temperature on a Nicolet 5700 FT-IR spectrometer in the range of wave numbers 400–4000  $\text{cm}^{-1}$  at a resolution  $4 \text{ cm}^{-1}$  (number of scans, 32). In situ FT-IR spectra for CO or/and NO molecules filled in IR cell (equipped with KBr windows) were recorded at various target temperatures as background for each test. The CZ support and Cu-CZ catalysts wafers (about 10 mg) were mounted in a quartz IR cell and pretreated for 1 h at  $100^\circ\text{C}$ , followed by flowing  $\text{N}_2$  atmosphere. After cooled to room temperature, the sample wafers were exposed to the stream of  $\text{CO-N}_2$  (10% of CO of volume) or/and  $\text{NO-He}$  (10% of NO by volume) flow at a rate of  $5.0 \text{ ml min}^{-1}$  for 30 min. Desorption/reaction studies were performed by heating the adsorbed species at different temperatures. All of the presented spectra were obtained by subtraction of the corresponding background reference.

#### 2.2.2. X-ray diffraction (XRD) measurement

XRD patterns were recorded on a Philips X'pert Pro diffractometer using Ni-filtered  $\text{Cu K}\alpha$  radiation ( $\lambda = 0.15418 \text{ nm}$ ). The X-ray tube was operated at  $40 \text{ kV}$  and  $40 \text{ mA}$ . The mean grain sizes ( $D_\beta$ ) of the  $\text{CeO}_2$ ,  $\text{t-ZrO}_2$  and CZ samples were determined from line-broadening measurements on the (1 1 1) plane, using the Scherrer equation,  $D_\beta = K\lambda/\beta \cos \theta$ , where  $\lambda$  was the synchrotron wavelength,  $K$  was the particle shape factor, taken as 0.94 for spherical particles,  $\beta$  was the full-width at half maximum height (FWHM) in radians. The XRD patterns for  $x\text{Cu-CZ}$  catalysts after reaction at  $250$  and  $350^\circ\text{C}$  were recorded by the same condition.

#### 2.2.3. Laser Raman spectroscopy (LRS) measurement

LRS spectra were collected on a Jobin-Yvon (France–Japan) T64000 type Laser Raman spectroscopy using  $\text{Ar}^+$  laser beam. The Raman spectra were recorded with an excitation wavelength of  $532 \text{ nm}$  and the laser power of  $300 \text{ mW}$ .

#### 2.2.4. $H_2$ -temperature programmed reduction (TPR) measurement

TPR was carried out in a quartz U-tube reactor with a thermal conduction detector (TCD) and  $\text{H}_2\text{-Ar}$  mixture (7.3% of  $\text{H}_2$  by

volume) as reductant. 50 mg of sample was used for each measurement. Before switched to the  $\text{H}_2\text{-Ar}$  stream, the sample was pretreated in a  $\text{N}_2$  stream at  $100^\circ\text{C}$  for 1 h. TPR started from room temperature at a rate of  $10^\circ\text{C min}^{-1}$ . These CuO–CZ catalysts were pretreated in  $\text{N}_2$  stream for 1 h and reacted at  $150$ ,  $250$  and  $350^\circ\text{C}$  for 20 min. These used catalysts were first cooled to room temperature in the flowing reactants, and then quickly transferred to U-tube reactor. The same procedure was then operated for TPR results.

### 2.3. Catalytic activity tests

The catalytic activity and selectivity of the catalysts were evaluated under steady state, involving a feed steam with a fixed composition, NO 5%, CO 10% and He 85% by volume as diluents. A quartz tube with a requisite quantity of catalyst (50 mg) was used. The catalysts were pretreated in  $\text{N}_2$  stream at  $100^\circ\text{C}$  for 1 h and then cooled to room temperature, after that, the mixed gas was switched on. The reactions were carried out at different temperatures with a space velocity of  $12,000 \text{ h}^{-1}$ . Two volumes (diameter 3 mm and length 1.75 m, respectively;  $T = 40^\circ\text{C}$ ) and

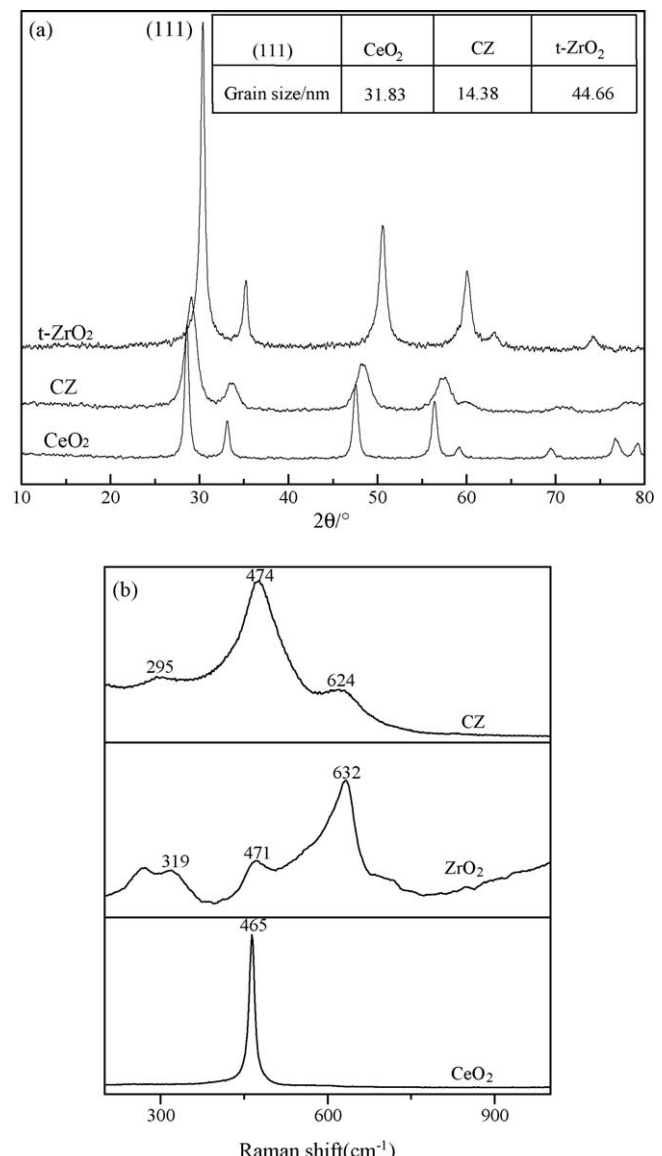


**Fig. 1.** XRD (a) and Raman (b) results of  $\text{CeO}_2$ ,  $t\text{-ZrO}_2$  and CZ samples, the grain size of these samples was listed in the inset table.

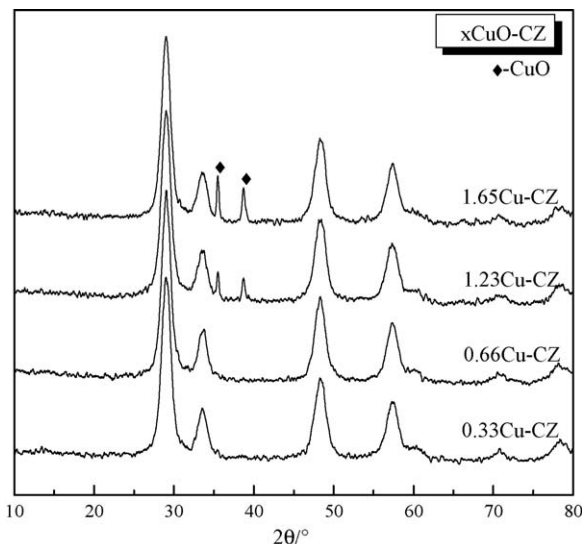


**Fig. 2.** XRD patterns of xCu-CZ catalysts with different CuO loading amounts.

thermal conduction detections ( $T = 100\text{ }^{\circ}\text{C}$ ) were used for the purpose of analyzing the production, volume A with Paropak Q for separating  $\text{N}_2\text{O}$  and  $\text{CO}_2$ , and volume B, packed with 5A and 13X molecule sieve (40–60 M) for separating  $\text{N}_2$ , NO and CO.

### 3. Results and discussion

#### 3.1. XRD and Raman results

The XRD patterns for  $\text{CeO}_2$ , tetragonal  $\text{ZrO}_2$  and CZ samples were shown in Fig. 1a. Compared with  $\text{CeO}_2$  and t- $\text{ZrO}_2$ , the diffraction peaks of CZ sample were broader due to crystallite nanodimensions effect [20,21], as evidenced by the grain size of these samples in the insert table, the grain size of CZ was much smaller than that of  $\text{CeO}_2$  and t- $\text{ZrO}_2$ . Their positions were located in between those corresponding peaks for ceria and t-zirconia, which indicated that zirconium ions had been successfully doped into the lattice of ceria [21] and CZ solid solution maintained the fluorite-type structure [24]. In Raman spectra (Fig. 1b), the band at  $\sim 465\text{ cm}^{-1}$  for  $\text{CeO}_2$  and the band at  $\sim 471\text{ cm}^{-1}$  were attributed to

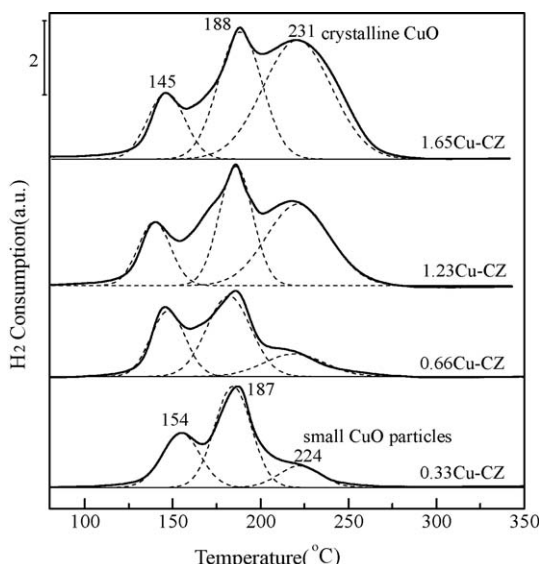


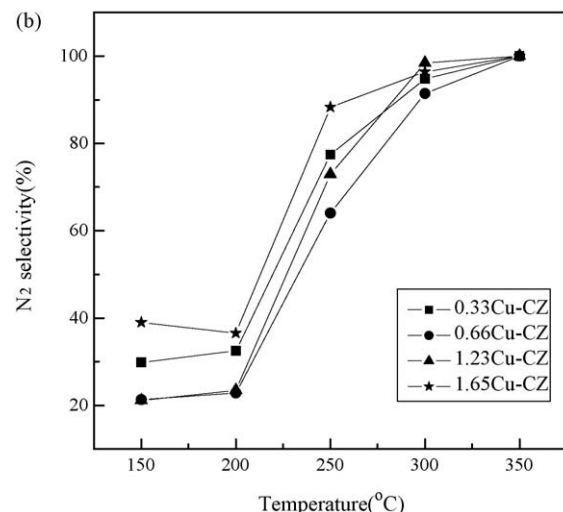
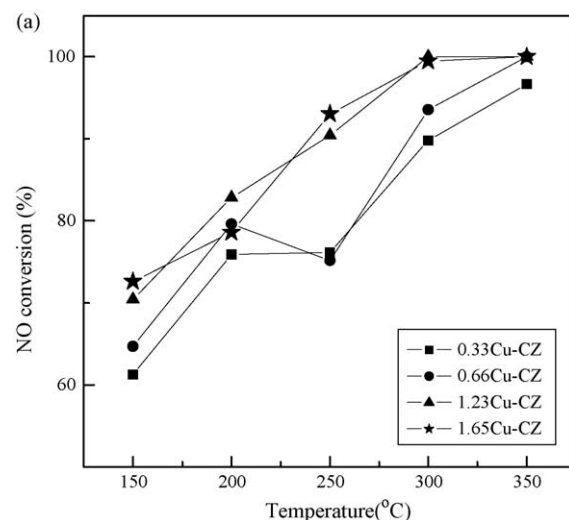
**Fig. 3.** TPR profiles of various xCu-CZ catalysts with different CuO loading amounts.

the  $\text{F}_{2g}$  vibration of fluorite-type lattice. For CZ sample, this band shifted to  $\sim 474\text{ cm}^{-1}$ . In addition, two new bands at  $295$  and  $624\text{ cm}^{-1}$  were observed, which should be related to the lattice contraction from the zirconium ions insertion [20].

In Fig. 2, for those samples with low CuO loading amounts ( $\leq 0.66\text{ mmol}/100\text{ m}^2\text{ CZ}$ ), no characteristic peaks of crystalline CuO were detected, which suggested that copper oxide species were highly dispersed on the surface of CZ support. When the copper oxide content increased, the diffraction peaks for crystalline CuO appeared and their intensities became much stronger with the copper oxide loadings. This was because the copper oxide loading was more than the monolayer dispersion capacity of CZ solid solution ( $1.07\text{ mmol}/100\text{ m}^2\text{ CZ}$ ).

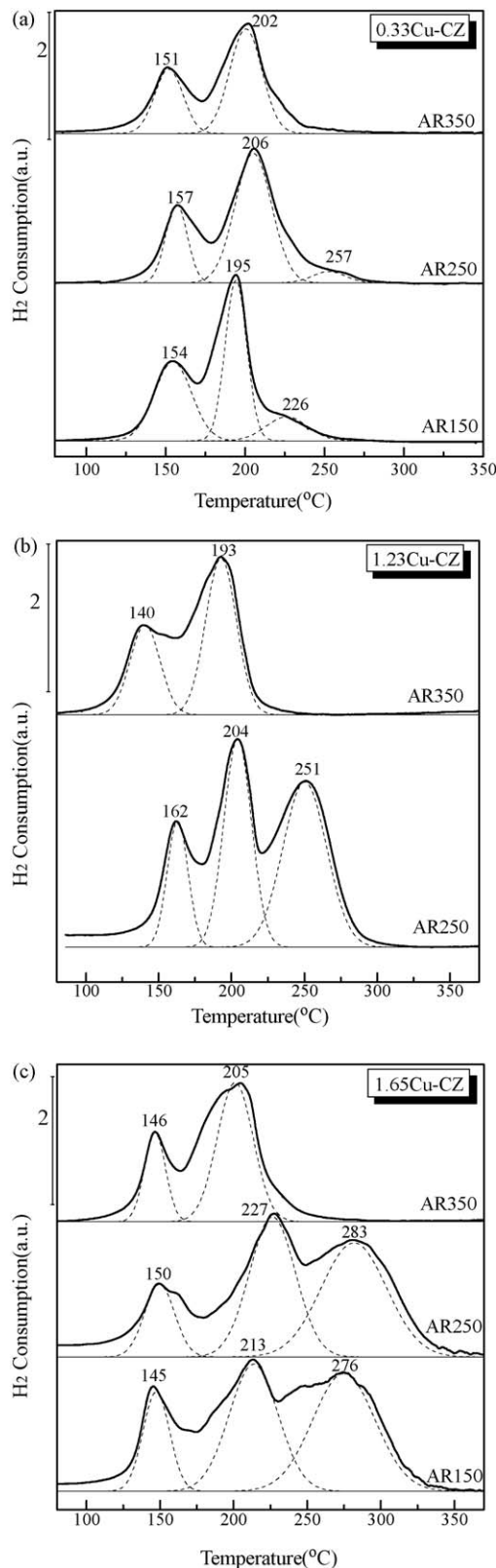
#### 3.2. $\text{H}_2$ -TPR results

Fig. 3 shows the TPR results for these xCu-CZ samples. For 0.33Cu-CZ sample, the two peaks at  $\sim 154$  and  $\sim 187\text{ }^{\circ}\text{C}$  were assigned to the stepwise reduction of surface dispersed CuO species, i.e.,  $\text{Cu}^{2+} \rightarrow \text{Cu}^+$  and  $\text{Cu}^+ \rightarrow \text{Cu}^0$  [9,10,12,27], while the small one at  $\sim 224\text{ }^{\circ}\text{C}$  might be related to small CuO particles. Moreover, for 1.65Cu-CZ sample, three peaks appeared. Two peaks at low temperature were also attributed to the stepwise reduction



**Fig. 4.** Results of (a) NO conversion (%) and (b)  $\text{N}_2$  selectivity (%) over xCu-CZ catalysts with different CuO loadings as a function of reaction temperatures. Feed composition: NO 5%, CO 10% and He 85% by volume,  $\text{GV} = 12,000\text{ h}^{-1}$ .

of surface dispersed CuO species, and the other one at  $\sim 231$  °C was represented by the reduction of crystalline CuO [27], which were in agreement with XRD results. In addition, it was noteworthy that these reduction peaks of  $x$ Cu-CZ samples should be connected to



**Fig. 5.** TPR results of  $H_2$  reaction over  $x$ Cu-CZ after reaction at 150, 250 and 350 °C. (a) 0.33Cu-CZ; (b) 1.23Cu-CZ; (c) 1.65Cu-CZ. These used catalysts at different temperatures were denoted as AR150, 250 and 350.

surface layer reduction of ceria. The  $H_2$  consumption (data not shown) of fresh samples was higher than what was needed for the stoichiometric reduction of CuO to  $Cu^0$ . This excess hydrogen uptake should be due to the ceria surface oxygen reduction [38–44]. As reported elsewhere, two reduction peaks were registered in the TPR profiles of pure ceria [47] and ceria-zirconia samples prepared by coprecipitation [20,23]; the low temperature peak at about 500 °C was assigned to ceria surface layers reduction, and the high temperature one (800 °C and above) was related to the bulk reduction of ceria. The promoted reduction behavior of ceria in this work should be closely related to the Zr introduction and the interaction between copper species and ceria [20,23,40,43,44].

### 3.3. Catalytic activity/selectivity results

The NO conversion and  $N_2$  selectivity results as a function of temperature were given in Fig. 4 for  $x$ Cu-CZ catalysts. At 150–200 °C, NO conversion (Fig. 4a) reached 60–75% at a space velocity of 12,000  $h^{-1}$  over 0.33Cu-CZ catalyst, and it increased with the temperature. However, the  $N_2$  selectivity (Fig. 4b) at 150–200 °C was very low. When the temperature increased further, the  $N_2$  selectivity increased dramatically and reached 100% at 300 °C. In addition, it was interesting that the increase of copper oxide loading from 0.33 to 1.65 mmol/100  $m^2$ CZ did not lead to the corresponding enhancement of NO conversion, which implied that the highly dispersed copper oxide species might be the main active components for this reaction according to the XRD and TPR results [9,11,45]. The difference in  $N_2$  selectivity at low and high temperatures suggested that different mechanisms possibly worked at low and high temperatures [17–19,46], which might be resulted from the change of active species at high temperature [11–13]. TPR and XRD measurements, which are simple and powerful tool for distinguishing between surface phases of copper–ceria related catalysts, were combined to track whether the  $x$ Cu-CZ catalysts were changed during the reaction process.

In Fig. 5, for three  $x$ Cu-CZ samples after reaction at 150 and 250 °C, the reduction peaks and  $H_2$  consumption were similar to that of before reaction, indicating that these catalysts did not change below 250 °C [40,42]. However, when the 0.33Cu-CZ sample was used at 350 °C, the reduction peak for small CuO particles disappeared. For 1.23Cu-CZ and 1.65Cu-CZ samples, the reduction peak for crystalline CuO also disappeared after reaction at 350 °C. In addition, the reduction temperature for those second peaks increased and the  $H_2$  consumption decreased (not shown).

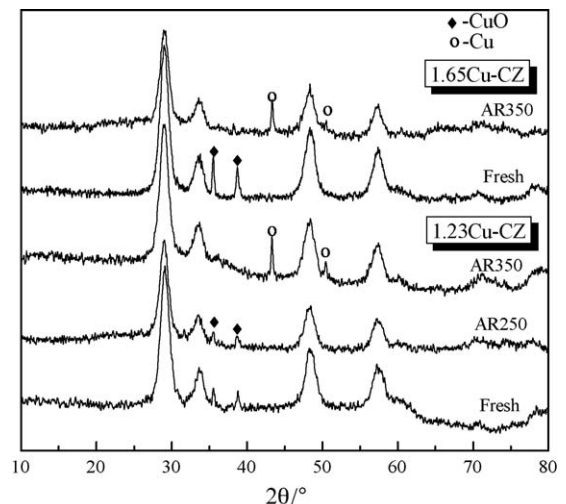


**Fig. 6.** XRD patterns of fresh  $x$ Cu-CZ catalysts and those after reaction at 250 and 350 °C.

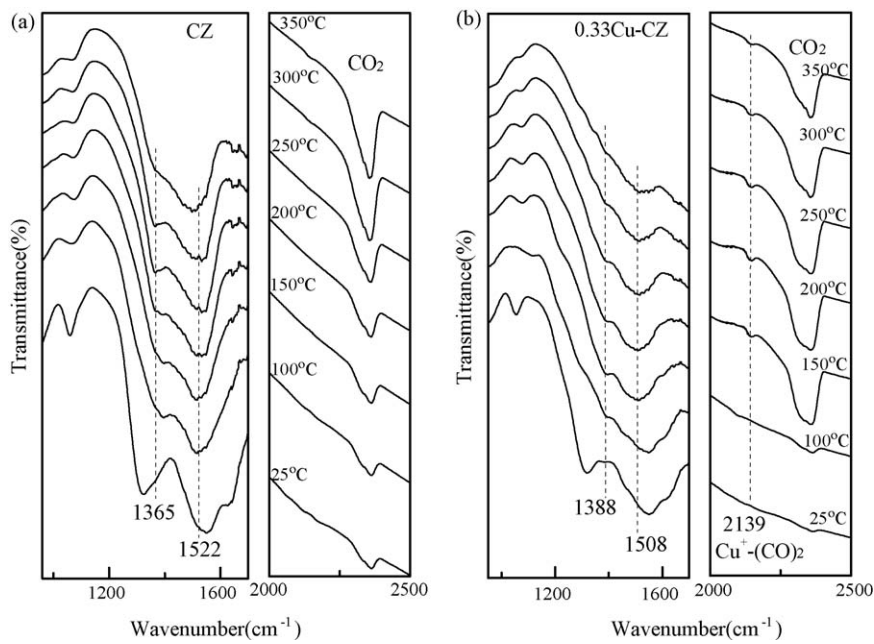


**Fig. 7.** In situ FT-IR results of CO (10% in volume) interaction with (a) CZ and (b) 0.33Cu-CZ catalysts from 25 to 350 °C at a heating rate 10 °C min<sup>-1</sup>.

These results revealed that partial copper oxides were reduced to low valence state and surface oxygen of ceria was consumed above 250 °C. This lack of reproducibility in reduction behavior of these catalysts after the use at high temperature implied the change in the morphology and oxidation state of copper species on CZ support occurred during the first reaction process [44]. XRD results in Fig. 6 for 1.23Cu-CZ and 1.65Cu-CZ samples suggested that the crystalline CuO was still present after reaction at 250 °C, while it was reduced into metal copper by CO at 350 °C. These results further confirmed that the surface copper oxide had been changed to Cu<sup>+</sup>/Cu<sup>0</sup> species at higher than 250 °C, which should be responsible for the N<sub>2</sub> selectivity enhancement [34,36].

### 3.4. FT-IR results of CO or/and NO interaction with Cu-CZ catalysts

#### 3.4.1. CO interaction with CZ and 0.33Cu-CZ

As reported previously [32], for the adsorption of CO on CuO/ $\gamma$ -Al<sub>2</sub>O<sub>3</sub> catalysts, the main bands at 2057, 2116 and 2177  $\text{cm}^{-1}$  could be observed after the catalysts treated by CO at 250 °C, which were assigned to CO bonded to Cu<sup>+</sup> species dispersed on the surface of  $\gamma$ -Al<sub>2</sub>O<sub>3</sub>. The similar bands can also be observed during the temperature increase because of the reduction of the dispersed Cu<sup>2+</sup> to Cu<sup>+</sup> species. As shown in Fig. 7, for CZ support, the band at 2360  $\text{cm}^{-1}$  for CO<sub>2</sub> could be detected and its intensity gradually increased with temperature increasing from 25 to 350 °C,

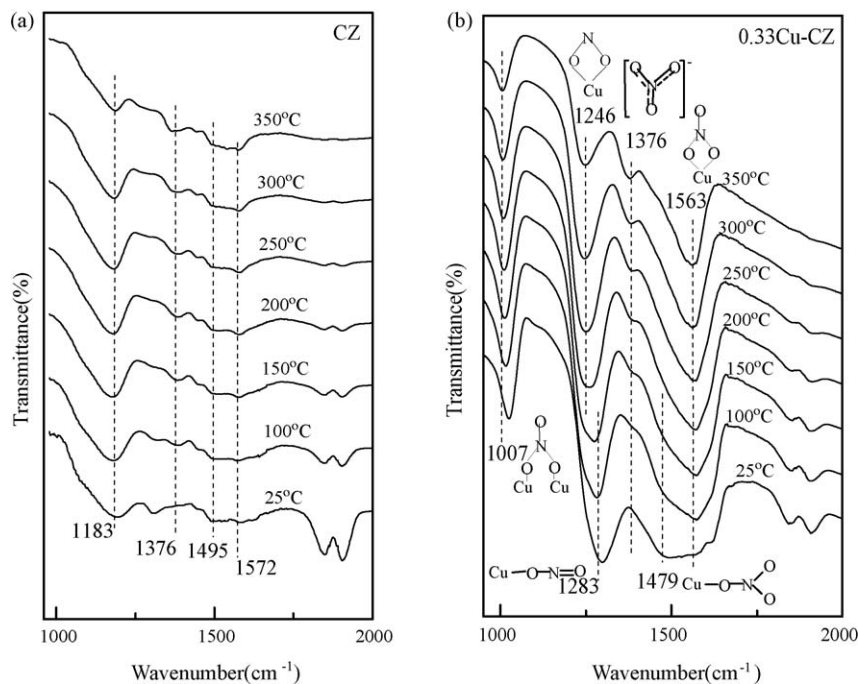


**Fig. 8.** In situ FT-IR results of NO (10% in volume) interaction with (a) CZ and (b) 0.33Cu-CZ catalysts from 25 to 350 °C at a heating rate 10 °C min<sup>-1</sup>, the models of these adsorbed NO species were displayed in the figure.

indicating that CZ support could be reduced by CO during the heating treatment. The formation of  $\text{CO}_2$  could be due to reaction of CO with active oxygen originating from CZ carrier [1,3,5,25]. Moreover, two bands at 1365 and 1522  $\text{cm}^{-1}$  were assigned to the adsorption of surface carbonates [33], and their intensities kept stable independent of temperature. Therefore, it was reasonable to assume that the surface basic properties of CZ support affected the CO activation which might result in the influence on the activity of NO reduction [5]. Dramatically, regarding 0.33Cu-CZ sample, a distinct broad band at 2360  $\text{cm}^{-1}$  and a tiny one at 2139  $\text{cm}^{-1}$  simultaneously appeared when the temperature was raised to 150 °C, which were attributed to the characteristic vibration of  $\text{CO}_2$  and  $(\text{CO})_2\text{-Cu}^+$ , respectively. These results suggested that the adsorption of CO molecules on 0.33Cu-CZ led to the reduction of part of surface dispersed CuO to  $\text{Cu}^+$  species [32,36], which further supported the TPR and activity test results. On the other hand, the bands at 1365 and 1522  $\text{cm}^{-1}$  for adsorbed carbonates on CZ shifted to 1388 and 1508  $\text{cm}^{-1}$  on 0.33Cu-CZ sample. These bands disappeared at 350 °C, suggesting that surface copper oxide species influenced the stability of carbonate on CZ support.

#### 3.4.2. NO interaction with CZ and 0.33Cu-CZ

Fig. 8 shows the in situ FT-IR spectra of adsorbates produced from flowing NO over CZ support and 0.33Cu-CZ from 25 to 350 °C. In view of CZ support, the first strong band at 1183  $\text{cm}^{-1}$  was ascribed to anionic nitrosyl,  $\text{NO}^-$  [6,31,35]. The second one at 1376  $\text{cm}^{-1}$  was from the typical adsorption of free  $\text{NO}_3^-$  ions and the band at 1572  $\text{cm}^{-1}$  was due to the adsorption of the  $\nu(\text{N}=\text{O})$  mode of surface bidentate nitrate, and NO weakly chemisorbed as a form of  $\text{M}-(\text{NO})^+$  on the surface of support presented the bands at 1847 and 1911  $\text{cm}^{-1}$ . Therefore, NO was oxidized by lattice oxygen from CZ support [26,31]. This could be explained by the strong oxygen storage and release properties of ceria-zirconia solid solution where surface oxygen could promote the following reaction:  $\text{NO} + \text{O}_2 = \text{NO}_2$  [35]. In addition, these bands were difficult to decompose even at 350 °C, indicating these species were stable on CZ support. For 0.33Cu-CZ sample, a series of new bands in the 1000–1650  $\text{cm}^{-1}$  region were observed instead. As reported elsewhere [1,2,5,6,16,28–31,37], bridging bidentate nitrate exhibited a remarkable  $\text{NO}_2$  symmetric vibration band at 1007  $\text{cm}^{-1}$  and a weak  $\text{N}=\text{O}$  stretching model at 1620  $\text{cm}^{-1}$ . Chelating bidentate nitrate gave a significant NO vibration fraction

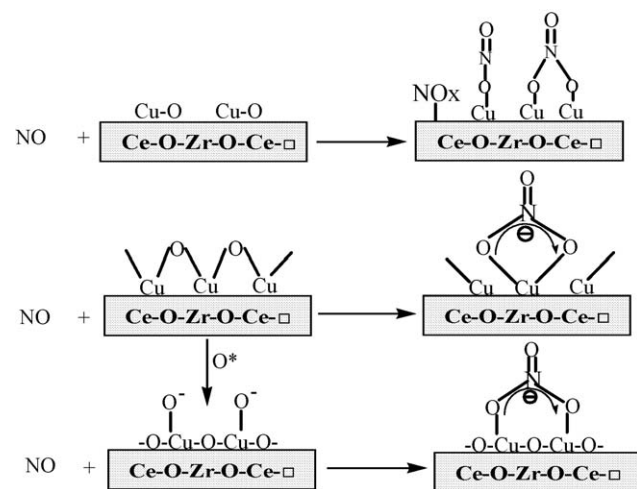


**Fig. 9.** The schematic diagram of NO interaction with copper oxide species supported on CZ from in situ FT-IR spectroscopy.

at 1563  $\text{cm}^{-1}$ ; monodentate nitrate showed a  $\text{NO}_2$  asymmetric vibration band at 1479  $\text{cm}^{-1}$ . Moreover, linear nitrite ( $\text{Cu}^{2+}-\text{O}-\text{N}=\text{O}$ ) had the  $\text{NO}_2$  asymmetric vibration band at 1283  $\text{cm}^{-1}$ . Along this line, these results demonstrated that NO molecules had preferentially interacted with the dispersed copper oxide, thus formed several kinds of nitrate or nitrite-like species, which were dependent on the configurations of surface copper oxide [28,30,34,36]. The possible reactions were displayed in Fig. 9. The strong interaction between the dispersed copper oxide and CZ support might lead to the active oxygen migration from CZ to copper sites [7].

During the heating process, the adsorbed linear nitrite at 1283  $\text{cm}^{-1}$  had gradually red shifted to 1246  $\text{cm}^{-1}$ , which was associated with chelating nitro species. Correspondingly, the monodentate nitrate at 1479  $\text{cm}^{-1}$  [2,16] blue shifted to 1563  $\text{cm}^{-1}$  and disappeared at 150 °C. This phenomenon suggested that both linear nitrite and monodentate nitrate were not thermally stable and readily to transform to other forms or decompose. Additionally, a new band appeared at 1376  $\text{cm}^{-1}$  when the temperature reached 150 °C, which was corresponded to the  $\text{NO}_2$  stretching vibration of distorted ionic nitrate [35]. The

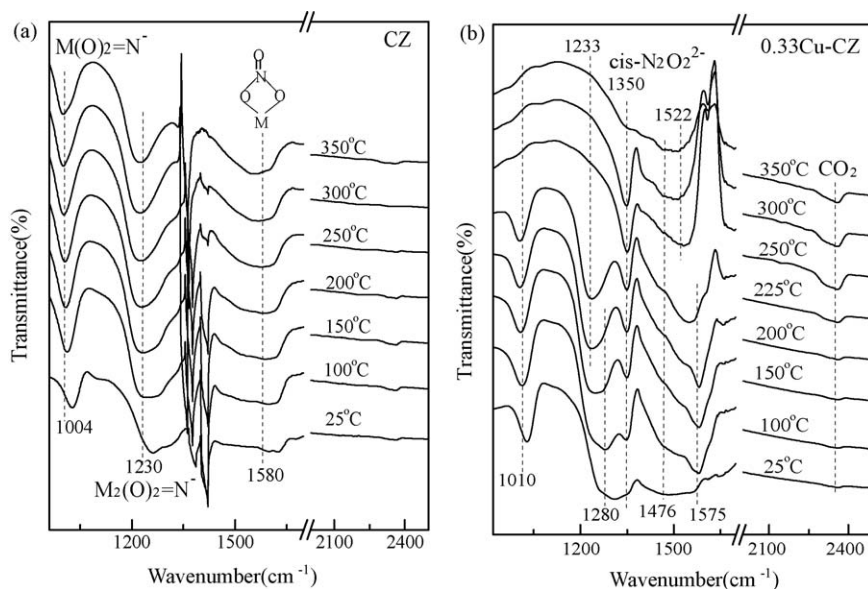


**Fig. 10.** In situ FT-IR results of CO and NO (10% in volume) co-interaction with (a) CZ and (b) 0.33Cu-CZ catalysts from 25 to 350 °C at a heating rate 10 °C min<sup>-1</sup>.

formation of these oxidized nitric oxide species, such as bridging bidentate, chelating bidentate, monodentate nitrate and  $\text{NO}_3^-$  ions on copper oxide species, might be related to the active lattice oxygen from CZ support [25,26,35].

#### 3.4.3. CO and NO co-interaction with CZ and 0.33Cu-CZ

In order to further approach this surface reaction mechanism, CO and NO co-adsorption FT-IR were recorded under the simulating reaction conditions, as shown in Fig. 10. CO and NO co-interaction with CZ produced three types of NO adsorption species on the surface. The bands at 1004 and 1230  $\text{cm}^{-1}$  could be attributed to the adsorption of chelating nitrite ( $\text{M}-(\text{O})_2=\text{N}^-$ ) and

symmetric stretch of bridge nitrites ( $\text{M}_2(\text{O})_2=\text{N}^-$ ), respectively. The broad one at 1580  $\text{cm}^{-1}$  was belonging to the adsorption of chelating bidentate nitrate [5,35]. These species were very thermally stable even at 350 °C. During the heating process, neither  $\text{CO}_2$  nor carbonates could be detected, which might be resulted from the preferential adsorption of NO on CZ support. As a result, CO adsorption on CZ support was inhibited [1,2,7]. The adsorption of NO on CZ support should be attributed to surface oxygen vacancies in ceria [4,13,15,36,38].

Subsequently, the same results could be found on 0.33Cu-CZ sample, i.e., NO preferentially interacted with 0.33Cu-CZ compared with CO due to its strong adsorption ability. These results were

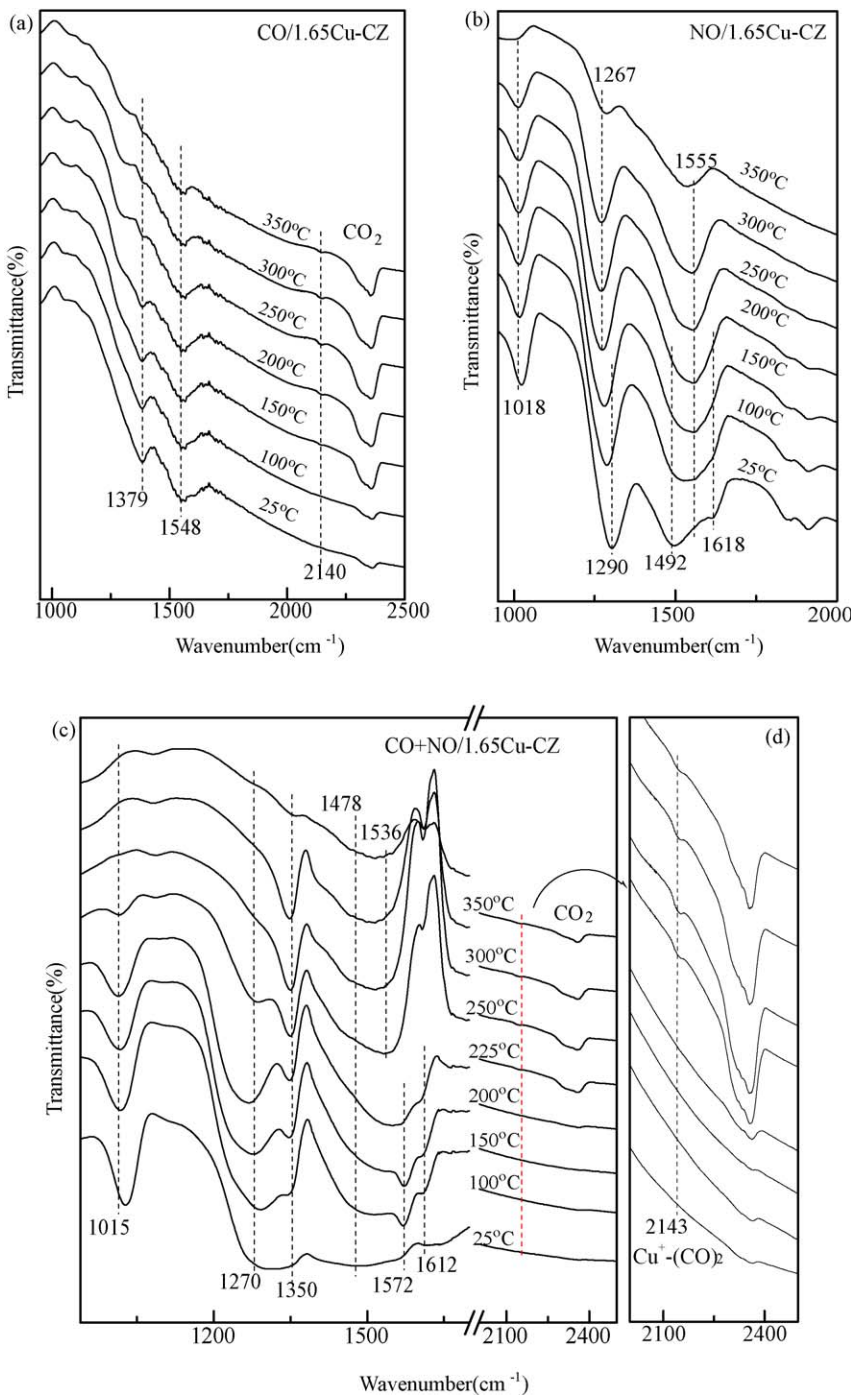


**Fig. 11.** In situ FT-IR results of CO or/and NO (10% in volume) interaction with 1.65Cu-CZ catalyst from 25 to 350 °C at a heating rate 10 °C min<sup>-1</sup>, (a) CO; (b) NO; (c) CO + NO; (d) part of the wavenumber from 2000 to 2500  $\text{cm}^{-1}$ .

**Table 1**

The related FT-IR bands formed upon the adsorption of CO or/and NO on CZ and xCu-CZ samples at different temperatures.  $\nu_{as}$ : asymmetric stretching vibration;  $\nu$ : symmetric stretching vibration; n.f.: not found; M = Ce<sup>4+</sup>, Zr<sup>4+</sup>.

Samples	CO <sub>x</sub> /NO <sub>x</sub> species	Band position (cm <sup>-1</sup> )			Assignments
		CO	NO	NO + CO	
Cu-CZ	Bridging bidentate nitrate		1620	1610	$\nu(N=O)$
			1007	1010	$\nu(NO_2)$
	Chelating nitro		1246	1233	$\nu(NO_2)$
	Chelating bidentate nitrate		1563	1575	$\nu(N=O)$
				1522	
	Linear nitrite		1283	1280	$\nu_{as}(NO_2)$
	Monodentate nitrate		1479	1476	$\nu_{as}(NO_2)$
	Free nitrate ion		1376	n.f.	$\nu_{as}(NO_2)$
	Cis-hyponitrites (N <sub>2</sub> O <sub>2</sub> <sup>2-</sup> )		n.f.	1350	$\nu(N-N)$
	Surface carbonates	1388	n.f.	n.f.	$\nu_s(C-O)$
		1508			$\nu_{as}(CO_2^-)$
	(CO) <sub>2</sub> -Cu <sup>+</sup>	2139	n.f.	2143	(C-O)
CZ	CO <sub>2</sub>	2360		2360	
	Surface carbonates	1365	n.f.		$\nu_s(C-O)$
		1522			$\nu_{as}(CO_2^-)$
	Chelating bidentate nitrate		1572	1580	
	M <sub>2</sub> (O) <sub>2</sub> =N <sup>-</sup> nitrites	n.f.	1183	1230	$\nu(N-O)$
	M(O <sub>2</sub> )=N <sup>-</sup>		n.f.	1004	
	Weak gas phase M-(NO) <sup>+</sup>		1847	n.f.	$\nu(NO)$
			1911		

supported by the results about CO and NO adsorption on Ru-PtNaY [2] from Martins et al. However, the NO adsorption species on 0.33Cu-CZ rearranged when the temperature increased to 150 °C. The band at 1280 cm<sup>-1</sup> for linear nitrite gradually disappeared with the appearance of the band at 1233 cm<sup>-1</sup> for chelating nitrite and the cis-hyponitrites N<sub>2</sub>O<sub>2</sub><sup>2-</sup> species at 1350 cm<sup>-1</sup> [37]. Additionally, the band for chelating bidentate nitrate at 1575 cm<sup>-1</sup> was formed during the initial stage, as well as monodentate nitrate at 1476 cm<sup>-1</sup>. They were stable below 250 °C. However, these adsorbed species as intermediates, including bridging/chelating bidentate nitrate and chelating nitrite, entirely vanished at the expense of CO oxidation when the temperature reached 250 °C. Correspondingly, the band at 2360 cm<sup>-1</sup> for CO<sub>2</sub> and a new band at 1522 cm<sup>-1</sup> were obtained, which might be the signal for the adsorption of NO on the reduced copper oxide. In particular, the dominant one (N<sub>2</sub>O<sub>2</sub><sup>2-</sup>) remained steady up to 300 °C, but negligible amount was left up to 350 °C. With respect to above results, it was inferred that these adsorbates had readily reacted with CO during the heating process.

#### 3.4.4. Comparison between CO or/and NO interaction with 1.65Cu-CZ

Fig. 11 shows the FT-IR results of CO or/and NO interaction with 1.65Cu-CZ. In Fig. 11a, the bands at 1379 cm<sup>-1</sup> and 1548 cm<sup>-1</sup> were attributed to the adsorption of the symmetric C-O stretching mode [33] and  $\nu_{as}(CO_2^-)$  of bidentate format [5] on CZ support. A small band at 2140 cm<sup>-1</sup> should be related to the adsorption of CO species on the reduced copper oxide. These results suggested that CO preferred to adsorb on CZ support rather than dispersed copper oxide [1,5]. For NO adsorption on 1.65Cu-CZ (Fig. 11b), bidentate and linear nitrites (1267 and 1290 cm<sup>-1</sup>) and various types of adsorption nitrates (several bands in the range 1000–1700 cm<sup>-1</sup>) were formed on the sample surface. These surface species were similar to that over the 0.33Cu-CZ, which meant that the crystalline CuO might make little donation to the formation of new NO adsorption species. In addition, both the adsorbed carbonates, nitrates and Cu<sup>+</sup> carbonyls were stable even at 350 °C.

Amusingly, for CO and NO co-adsorption on 1.65Cu-CZ sample (Fig. 11c), the adsorbed species differed expressively on their features and thermal stability. A new band at 1350 cm<sup>-1</sup> for cis-N<sub>2</sub>O<sub>2</sub><sup>2-</sup> appeared with the temperature increasing. The band at

1555 cm<sup>-1</sup> for bidentate nitrate was divided into two bands at 1572 and 1536 cm<sup>-1</sup> when the temperature reached 250 °C. The difference in vibration of the N-O bond should be attributed to the change of the oxidation state of adsorption sites [36]. In Fig. 11d, just when the temperature increased to 225 °C, a small band for (CO)<sub>2</sub>-Cu<sup>+</sup> species appeared and was stable to 350 °C. This was another evidence that the dispersed copper oxides were reduced to Cu<sup>+</sup> species during the NO reduction by CO process. Furthermore, these nitric oxide adsorbates, such as chelating nitrite, bridging and monodentate nitrate, completely disappeared at 250 °C. The dominant cis-N<sub>2</sub>O<sub>2</sub><sup>2-</sup> was dissolved at 350 °C. All these results indubitably disclosed that nitrates were the final form of adsorbed products on the catalyst surface [28] regardless of NO/CO adsorption or co-adsorption. The attributions of those bands mentioned above were listed in Table 1.

#### 3.5. Possible reaction mechanism over Cu-CZ catalysts

On the basis of above results, Fig. 12 showed the possible reaction proposal for NO reduction by CO over CuO-CZ catalysts under the current condition. When allowing NO and CO to react on the surface of CuO-CZ catalyst below 250 °C, NO was preferentially adsorbed on the CZ support and dispersed copper oxides, then several types of nitrite/nitrate species (bridging, monodentate nitrate and linear nitrite) were produced. They reacted with CO and mainly released N<sub>2</sub>O and CO<sub>2</sub> [17–19]. When the temperature increased to higher than 250 °C, the other NO adsorbates (cis-N<sub>2</sub>O<sub>2</sub><sup>2-</sup>, bidentate nitrate) were formed as final intermediates. Simultaneously, CO molecules interacted with surface copper

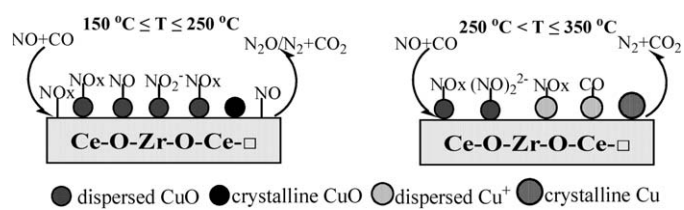


Fig. 12. Possible reaction mechanisms for NO reduction by CO over Cu-CZ catalyst below and above 250 °C.

oxide species and led to partial Cu<sup>2+</sup> reduced into Cu<sup>+</sup>/Cu<sup>0</sup> species [34,36]. The crystalline CuO was reduced to metal copper above 250 °C, while the dispersed CuO might be reduced to Cu<sup>+</sup> species that was active for CO adsorption. These unstable adsorbates were removed by active CO, and N<sub>2</sub> and CO<sub>2</sub> were acquired. The reducibility of Cu<sup>2+</sup> to Cu<sup>+</sup>/Cu<sup>0</sup> species should be related to the activity and N<sub>2</sub> selectivity of CuO-CZ catalysts.

#### 4. Conclusions

The dispersed copper oxide species on ceria-zirconia solid solution (Ce<sub>0.67</sub>Zr<sub>0.33</sub>O<sub>2</sub>) were the main active components for NO reduction by CO reaction. The catalysts were reduced by CO during the reaction process, which led to the dramatical increase in N<sub>2</sub> selectivity at high temperature. Hence, this reaction went through different mechanisms at low and high temperatures due to the change of active species.

FT-IR results suggested that: (1) CO was facilitated to activate by oxygen originating from CZ support, which led to surface carbonates formation, and partial dispersed copper oxides were reduced to Cu<sup>+</sup> species above 150 °C; (2) NO was captured by dispersed CuO and oxygen vacancies of ceria-zirconia solid solution, whereas crystalline CuO made little contribution for formation of new NO adsorbates; (3) NO was preferentially absorbed on CuO-CZ catalysts compared with CO, nitrates were the final adsorbed products on the catalysts surface. These adsorbed nitrate/nitrite species as active intermediates rearranged and reacted with CO above 250 °C.

#### Acknowledgements

The financial supports of the National Natural Science Foundation of China (Nos. 20573053 and 20873060) and the National 863 Program of China (Flue Gas SCR De-nitrification Technology and Demonstration in Large-scale Coal-fired Power Plant No. 2007AA061802) are gratefully acknowledged.

#### References

- [1] T. Chafik, D.I. Kondarides, X.E. Verykios, J. Catal. 190 (2000) 446–459.
- [2] R.L. Martins, M.A.S. Baldanza, M. Schamal, J. Phys. Chem. B 105 (2001) 10303–10307.
- [3] M. Fernández-García, Martínez-Arias, C. Belver, J.A. Anderson, J.C. Conesa, J. Soria, J. Catal. 190 (2000) 387–395.
- [4] A.B. Hungria, M. Fernández-García, J.A. Anderson, A. Martínez-Arias, J. Catal. 235 (2005) 262–271.
- [5] A. Kotsifa, D.I. Kondarides, X.E. Verykios, Appl. Catal. B: Environ. 72 (2007) 136–148.
- [6] T.D. Nakatsuji, T. Yamaguchi, N. Sato, H. Ohno, Appl. Catal. B: Environ. 85 (2008) 61–70.
- [7] A.B. Hungria, A. Iglesias-Juez, J.A. Anderson, J.C. Conesa, J. Soria, J. Catal. 206 (2002) 281–294.
- [8] E. Ozensoy, C. Hess, D.W. Goodman, J. Am. Chem. Soc. 124 (2002) 8524–8525.
- [9] Y.H. Hu, L. Dong, J. Wang, W.P. Ding, Y. Chen, J. Mol. Catal. A: Chem. 162 (2000) 307–316.
- [10] H.Y. Zhu, M.M. Shen, F. Gao, Y. Kong, L. Dong, Y. Chen, Catal. Commun. 5 (2004) 453–456.
- [11] S.D. Peter, E. Garbowksi, V. Perrichon, B. Pommier, M. Primet, Appl. Catal. A: Gen. 205 (2001) 147–158.
- [12] Y.H. Hu, L. Dong, M.M. Shen, D. Liu, J. Wang, Y. Chen, Appl. Catal. B: Environ. 31 (2001) 61–69.
- [13] X.Y. Jiang, L.P. Lou, Y.X. Chen, X.M. Zheng, J. Mol. Catal. A: Chem. 197 (2003) 193–205.
- [14] C.C. Pantazis, D.E. Petrakis, P.J. Pomonis, Appl. Catal. B: Environ. 77 (2007) 66–72.
- [15] B. Wen, M. He, Appl. Catal. B: Environ. 37 (2002) 75–82.
- [16] Y.W. Chi, S.S.C. Chuang, J. Catal. 190 (2000) 75–91.
- [17] I. Spassova, M. Khristova, D. Panayotov, D. Mehandjiev, J. Catal. 185 (1999) 43–57.
- [18] N.B. Stankova, M.S. Khristova, D.R. Mehandjiev, J. Colloid Interface Sci. 241 (2001) 439–447.
- [19] R. Nickolov, N.B. Stankova, M.S. Khristova, D.R. Mehandjiev, J. Colloid Interface Sci. 265 (2003) 121–128.
- [20] S. Letichevskya, C.A. Tellez, R.R. de Avillez, M.I.P. da Silva, Appl. Catal. B: Environ. 58 (2005) 203–210.
- [21] M.P. Yeste, J.C. Hernández, S. Bernal, G. Blanco, J.J. Calvino, Chem. Mater. 18 (2006) 2750–2757.
- [22] H.O. Zhu, J.R. Kim, S.K. Ihm, Appl. Catal. B: Environ. 86 (2009) 87–92.
- [23] J.R. Kim, W.J. Myeong, S.K. Ihm, Appl. Catal. B: Environ. 71 (2007) 57–63.
- [24] J.A. Rodriguez, J.C. Hanson, J.Y. Kim, G. Liu, J. Phys. Chem. B 107 (2003) 3535–3543.
- [25] M. Adamowska, S. Muller, P. Da Costa, A. Krzton, P. Burg, Appl. Catal. B: Environ. 74 (2007) 278–289.
- [26] M.W. Zhao, M.Q. Shen, J. Wang, J. Catal. 248 (2007) 258–267.
- [27] X.W. Li, M.M. Shen, X. Hong, H.Y. Zhu, F. Gao, L. Dong, J. Phys. Chem. B 109 (2005) 3949–3955.
- [28] Y.W. Chi, S.S.C. Chuang, J. Phys. Chem. B 10 (2000) 4673–4683.
- [29] J. Szanyi, J.H. Kwak, D.H. Kim, S.D. Burton, J. Phys. Chem. B 109 (2005) 27–29.
- [30] F. Prinetto, G. Ghiootti, I. Nova, L. Lietti, E. Tronconi, J. Phys. Chem. B 105 (2001) 12732–12745.
- [31] M. Kantcheva, E.Z. Ciftlikli, J. Phys. Chem. B 106 (2002) 3941–3949.
- [32] H.Q. Wan, Z. Wang, J. Zhu, X. Li, B. Liu, L. Dong, Appl. Catal. B: Environ. 79 (2008) 254–261.
- [33] M.M. Yung, Z.K. Zhao, M.P. Woods, U.S. Ozkan, J. Mol. Catal. A: Chem. 279 (2008) 1–9.
- [34] F. Amano, S. Suzuki, T. Yamamoto, T. Tanaka, Appl. Catal. B: Environ. 64 (2006) 282–289.
- [35] B. Azambre, L. Zenbouy, F. Delacroix, J.V. Weber, Catal. Today 137 (2008) 278–282.
- [36] A. Martínez-Arias, M. Fernández-García, A.B. Hungria, A. Iglesias-Juez, O. Gálvez, J.A. Anderson, J.C. Conesa, J. Soria, G. Munuera, J. Catal. 214 (2003) 261–272.
- [37] G. Qi, R.T. Yang, R. Chang, Appl. Catal. B: Environ. 51 (2004) 93–106.
- [38] L. Ilieva, G. Pantaleo, I. Ivanov, A.M. Venezia, D. Andreeva, Appl. Catal. B: Environ. 65 (2006) 101–109.
- [39] L. Ilieva, G. Pantaleo, I. Ivanov, R. Nedelyalkova, A.M. Venezia, D. Andreeva, Catal. Today 139 (2008) 168–173.
- [40] J. Beckers, G. Rothenberg, Dalton Trans. (2008) 6573–6657.
- [41] W.J. Shan, W.J. Shen, C. Li, Chem. Mater. 15 (2003) 4761–4767.
- [42] A. Pintar, J. Batista, S. Hočvar, J. Colloid Interface Sci. 285 (2005) 218–231.
- [43] P. Bera, K.R. Priolkar, P.R. Sarode, M.S. Hegde, S. Emura, R. Kumashiro, N.P. Lalla, Chem. Mater. 14 (2002) 3591–3601.
- [44] X.L. Tang, B.C. Zhang, Y. Li, Y.D. Xu, Q. Xin, W.J. Shen, Appl. Catal. A: Gen. 288 (2005) 116–125.
- [45] Y.Y. Xue, G.Z. Lu, Y. Guo, Y.L. Guo, Y.Q. Wang, Z.G. Zhang, Appl. Catal. B: Environ. 79 (2008) 262–269.
- [46] P. Granger, C. Dathy, J.J. Lecomte, L. Leclercq, M. Prigent, G. Mabilon, G. Leclercq, J. Catal. 173 (1998) 304–314.
- [47] B. Harrison, A.F. Diwell, C. Hallett, Plat. Met. Rev. 32 (1988) 73–83.